Residual Stresses in Friction Stir Processed (FSP) Nickel Aluminum Bronze

R. Ham-Su,[1] L.M. Cheng,[1] and M. A. Gharghouri[2]

[1] Defence Research & Development Canada – Atlantic, Dockyard Laboratory (Atlantic), Dartmouth, NS, Canada, B2Y 3Z7

[2] Canadian Neutron Beam Centre, National Research Council, Chalk River Laboratories, Chalk River, On, Canada K0J 1J0

Nickel aluminum bronze (NAB) is a copper-based alloy that is widely used for marine applications because of its excellent corrosion resistance, good fracture toughness, high damping capacity and good fatigue resistance [1, 2]. It is used for propellers and valves in the Canadian Navy's ships and in other Navies around the world. Cast NAB may contain shrinkage cavities and porosity. When these defects are large, they are traditionally repaired with arc welding, a high heat input process that introduces a filler metal into the casting, and can induce distortions in repaired components.

Friction Stir Processing (FSP) is based on friction stir welding (FSW), developed by TWI [3]. FSP is a solid-state thermomechanical processing method that can change the microstructure of metallic alloys and that has the ability to locally heal surface and subsurface casting defects. It has been found to homogenize and refine the microstructure of aluminum alloys with a resulting increase in ductility [4], and change the corrosion and fatigue properties of aluminum [5], [6]. Similarly, FSP refines the grain size of cast NAB; rotating-fatigue tests show that the processed region is more fatigue resistant, and Charpy impact tests show higher toughness at ambient temperatures and at –7°C [7].

In FSP, a turning probe is inserted into the workpiece, causing frictional heating. The probe is translated through the material, leaving a plasticized zone behind. FSP is currently being developed as a tool to heal casting defects and modify microstructures in as-cast NAB to improve its properties.

The present work is concerned with the residual stresses developed in a NAB plate due to Friction Stir Processing. This work was part of The Technical Cooperation Program (TTCP), wherein defence research organizations in TTCP nations collaborate on projects of common interest.

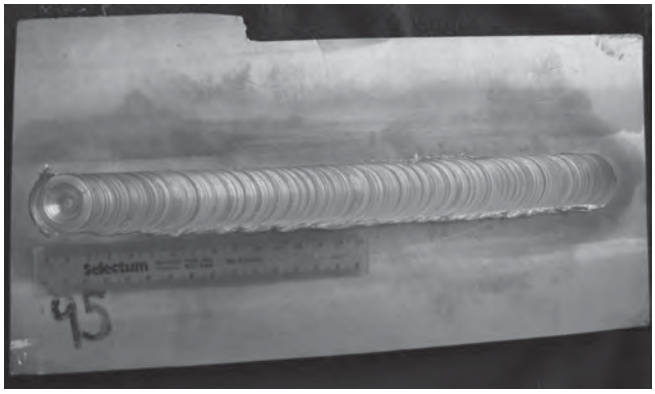

Fig 1. NAB cast plate. The FSP volume's top surface features semicircles that correspond to the rotating shoulder. This band of semicircles is surrounded by a blue-tinged region related to the high temperature reached in this region during FSP.

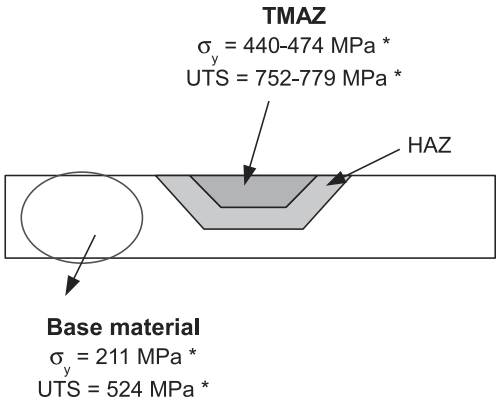

Fig 2. Mechanical properties in the TMAZ and in the parent material. * Data from Reference [7].

The specimen consisted of a NAB cast plate that was friction stir processed (Figure 1). The top surface of the plasticized zone or Thermomechanical Affected Zone (TMAZ) features semicircles that correspond to the rotating shoulder of the FSP probe. This band of semicircles is surrounded by a blue-tinged region which results from the heat generated during the process. The treated piece thus contains a TMAZ surrounded by a heat-affected zone (HAZ), surrounded in turn by as-cast material (Figure 2).

The NAB microstructure consisted of an α phase (fcc) matrix with κ precipitates. These precipitates are designated κ_i, κ_{ii}, κ_{iii}, and κ_{iv}. The compositions and structures of the matrix and the precipitates are listed in Table 1.

Residual lattice strains were measured using the L3 strain-scanning spectrometer. The sampling volume dimensions were 4 x 4 x (4-20) mm^3, depending on the direction of strain measurement. Lattice strains were measured in the longitudinal (*L*, parallel to the weld line), normal (*N*, perpendicular to the plane of the plate), and transverse (*T*, perpendicular to the weld line, in the plane of the plate) directions. The three corresponding normal residual stress components, σ_x, where x = (*L, T,* or *N*), were then calculated from the three measured strain components using the Generalized Hooke's Law:

$$\sigma_x = \frac{E}{1+\nu}\left[\varepsilon_x + \frac{\nu}{1-2\nu}\left(\varepsilon_L + \varepsilon_T + \varepsilon_N\right)\right], \quad for \quad x = [L, T, N]$$

where E is Young's modulus and ν is Poisson's ratio. Equation (1) assumes isotropic elasticity.

The copper {200}, {111}, {220}, and {311} reflections, and the

κ{110} reflection, were used for the measurements. A wavelength of 0.1513 nm was used for the Cu{220} and Cu{311} reflections, while a wavelength of 0.237 nm was used for the Cu{111}, Cu{200} and κ{110} reflections. The monochromatic beam was obtained using the {113} (λ = 0.1513 nm) and {115} (λ = 0.237 nm) reflections of a germanium single crystal monochromator.

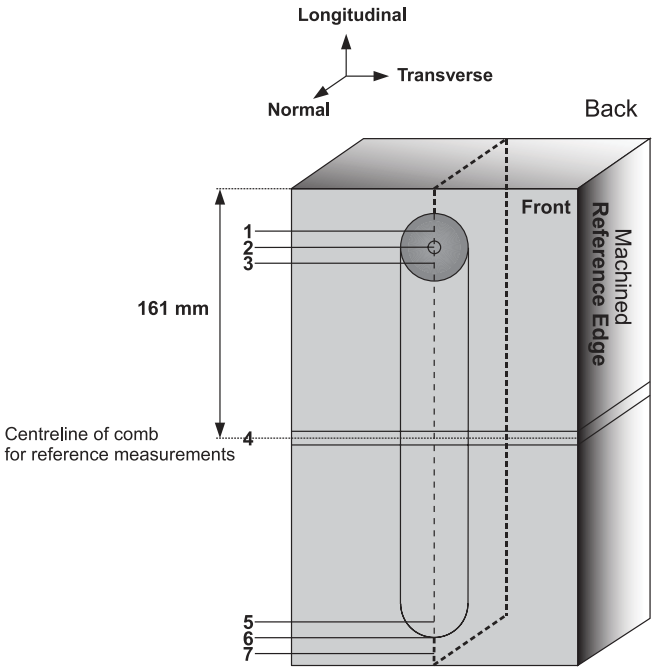

Fig 3. *Schematic of NAB specimen showing the reference surfaces, coordinate system, and measurement directions.*

The coordinate system, measurement directions, and reference surfaces used for the measurements are shown in Figure 3. Measurements were made at a series of locations along seven lines, numbered 1 – 7 in the figure. The location of a measurement along a line is given as the distance from the machined reference edge (the right edge in Figure 3). Measurements were made at 3 depths – at 4mm in from the front face (*F*), at mid-depth (*M*), and at 4 mm in from the back face (*B*). As shown in the figure, face *F* is the face that underwent friction stir processing.

In order to obtain reliable stress-free lattice spacings, it is usual to cut a small specimen out of the workpiece such that the Type I macrostresses are relaxed. It is important to recognize that the Type II and Type III microstresses may not be relaxed by this procedure. Thermomechanical processing can influence the microstructure of a material such that the equilibrium lattice spacing varies as a function of location. This is particularly relevant to processes involving a phase change such as fusion welding of a ferritic plain carbon steel. In the present case, it is unlikely that the composition of the material is strongly affected by the thermomechanical treatment. However, in order to investigate this issue, measurements were made on a comb of material extracted at line 4 (Figure 3) of the plate. The comb was extracted at DRDC Atlantic via electrical discharge machining, in order to eliminate the possibility of machining stresses. The removal of material between the teeth of the comb ensured the release of Type I macrostresses. The tooth dimensions were 4(*L*) x 4(*T*) x 20(*N*) mm^3 in the three measurement directions. Measurements were made on every tooth of the comb in the *L, T,* and *N* directions for all of the reflections used in this study.

The stress-free lattice parameter was obtained as the average from all of the longitudinal and transverse measurements for all of the lattice planes studied. The normal measurements were not used as they exhibited significant scatter, most likely due to the fact that Type I macrostresses were not effectively relaxed in this direction because of the comb geometry.

The stresses determined using the Cu{311} reflection for line 4 (Figure 3) are shown in Figures 4(a-c). The stresses were calculated using a Young's modulus of 130 GPa, and a Poisson's

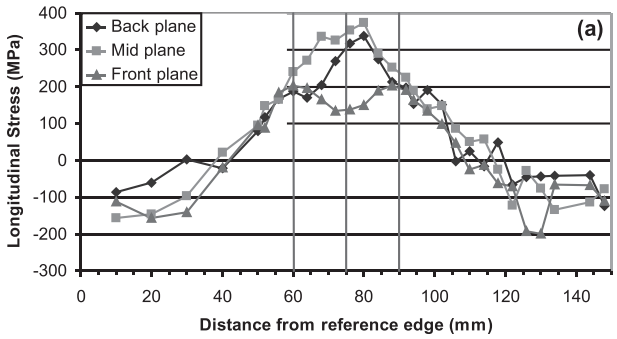

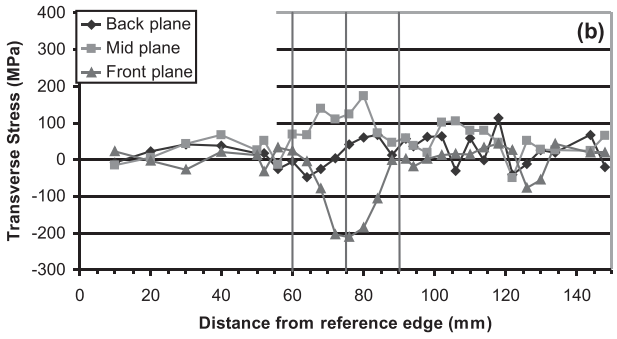

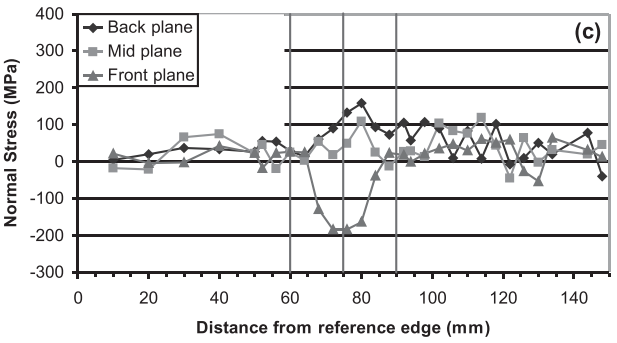

Fig 4. *Copper {311} stresses for a) the longitudinal, b) the transverse, and (c) the normal directions along line 4.*

ratio of 0.34, which are typical values for copper. The uncertainty in the calculated stresses is on the order of ±60 MPa.

The longitudinal stresses in Figure 4(a) show a clear tensile maximum at the centre of the FSP zone, with a dog-eared profile close to the front face. Balancing compressive stresses occur close to the plate edges. The tensile maximum at the front face is significantly weaker than at mid-depth and close to the back face.

The transverse stresses (Figure 4(b)) are weakly tensile close to the back face and at mid-depth, but show a compressive peak at the centre of the FSP zone close to the front face. A similar trend is exhibited by the normal stresses (Figure 4(c)). In the case of the transverse and normal stress components, it thus appears that the force balance imposed by equilibrium occurs from front to back rather from edge to edge. The plate is bent about its long axis, showing a slight concavity at the front face, which is consistent with the through-thickness variations exhibited by the transverse stresses.

In conclusion, residual stresses in a FSP-NAB plate were measured using neutron diffraction. The data will be used to validate numerical models of friction stir processing, and to understand the corrosion, biofouling, and mechanical properties of FSP-NAB.

Table 1: Structure and Composition of Matrix and κ-Precipitates in NAB[6].

Phase	Composition (approx.)	Structure	Lattice Parameter
α	Cu solid solution	fcc	3.64 Å
κ_i	Fe_3Al	$D0_3$	
κ_{ii}	Fe_3Al	$D0_3$	5.71 Å
κ_{iii}	NiAl	B_2	2.88 Å
κ_{iv}	Fe_3Al	$D0_3$	5.77 Å

References

[1] C.V. Hyatt; Defence Research Establishment Atlantic; Technical Memorandum 96/227, March 1997.
[2] J.A. Duma, Naval Engineers Journal, 87, 45 (1975).
[3] W.M. Thomas, E.D. Nicholas, J.C. Needham, M.G. Murch, P. emple-Smith, and C.J. Dawes; U.S. Patent No. 5460317, Oct. 1995.
[4] .B. Berbon, W.H. Bingel R.S. Mishra, C.C. Bampton and M.W. Mahoney, Scripta Mater., 44, 61 (2001).
[5] A. Merati, Corrosion and fatigue properties of friction stir welding in high strength aluminum alloy, NRC, Institute for Aerospace Research; in: Sedricks, A. J. Stress Corrosion Control in Friction Stir Welds in Al Alloys. The Technical Cooperation Program (TTCP) Report MAT TP-1/US/1/02, September 2002.
[6] P.S. Baburamani, et al, Fatigue of Friction Stir Welded Aluminium Alloys, TTCP Report TTCP-MAT-TP1-1-5-2006, May 2006.
[7] Julie Christodoulou, et al, Friction Sir Processing of Nickel Alumini um Bronze, TTCP Report TTCP-MAT-TP-1-2-2008, May 2008.